ECOLOGY

Spatial compartmentalization: A nonlethal predator mechanism to reduce parasite transmission between prey species

L. Gustavo R. Oliveira-Santos[1,2]*, Seth A. Moore[3], William J. Severud[1], James D. Forester[4], Edmund J. Isaac[3], Yvette Chenaux-Ibrahim[3], Tyler Garwood[1], Luis E. Escobar[5], Tiffany M. Wolf[1]

Predators can modulate disease transmission within prey populations by influencing prey demography and behavior. Predator-prey dynamics can involve multiple species in heterogeneous landscapes; however, studies of predation on disease transmission rarely consider the role of landscapes or the transmission among diverse prey species (i.e., spillover). We used high-resolution habitat and movement data to model spillover risk of the brainworm parasite (*Parelaphostrongylus tenuis*) between two prey species [white-tailed deer (*Odocoileus virginianus*) and moose (*Alces alces*)], accounting for predator [gray wolf (*Canis lupus*)] presence and landscape configuration. Results revealed that spring migratory movements of cervid hosts increased parasite spillover risk from deer to moose, an effect tempered by changes in elevation, land cover, and wolf presence. Wolves induced host-species segregation, a nonlethal mechanism that modulated disease emergence by reducing spatiotemporal overlap between infected and susceptible prey, showing that wildlife disease dynamics may change with landscape disturbance and the loss of large carnivores.

INTRODUCTION

Wildlife predators play a key role in the top-down cascade effect paradigm in ecology (*1*). Although predation drives trophic effects through the lethal removal of individuals within a population of prey, growing evidence highlights the importance of nonlethal effects through changes in prey behavior (*2*–*4*). Predator-induced changes in prey behavior are based on countermeasures to avoid predation (*5*). Nonetheless, nonlethal effects of predator presence can additionally influence food webs beyond what is expected with lethal effects alone (*6*, *7*).

Predators are known to also affect parasite transmission among prey, but research is dominated by studies of predator lethality over infectious hosts (*8*–*11*) [but see (*12*)]. The status quo in disease ecology theory proposes that predators' selective lethality on aged and diseased hosts is the main driver of transmission dynamics among prey populations (*12*–*14*). However, increased predator activity has been linked to decreased parasite transmission among prey without changes in prey abundance (*3*). For example, predator-driven nonlethal effects on parasite transmission may include behavioral changes, such as decreases in prey activity (*6*) and distribution (*15*, *16*), that reduce contact and transmission between infectious and susceptible individuals. Thus, we hypothesize that predators can also shape parasite transmission dynamics through nonlethal effects rather than the largely assumed lethal effects (*4*, *17*, *18*). These nonlethal effects may be more important in sustaining a healthy prey population by reducing parasite spillover to aberrant hosts, where the lethal removal of infected individual aberrant hosts would not necessarily affect ongoing transmission within a system (*11*). Further, transmission models generally assume that prey distribution is homogeneous with random movement of hosts and vectors (*15*). Therefore, the role of habitat configuration on prey distribution has been generally neglected in spillover models of wildlife (*19*, *20*). Accounting for habitat heterogeneity on prey distribution could offer new insights on the expectations of disease transmission in wildlife (*21*, *22*).

To better understand how nonlethal-predator effects and habitat configuration influence parasite transmission in a complex predator-prey system, we explored *Parelaphostrongylus tenuis* transmission from white-tailed deer (*Odocoileus virginianus*, hereafter deer) to moose (*Alces alces*) (*23*). Studies were conducted in northeastern Minnesota, United States, where moose populations have declined from about 10,000 individuals to less than 5000 in the past 15 years (*24*). Here, at least 23% of moose mortalities were affected by *P. tenuis*, where other causes of death included wolf predation, bacterial infection, accidents, hunter harvest, and calving complications (*25*). The *P. tenuis* nematode life cycle includes deer as the definitive host, terrestrial gastropods as intermediate host, and aberrant wildlife hosts (i.e., "spillover"), such as moose, elk (*Cervus canadensis*), caribou (*Rangifer tarandus*), and mule deer (*Odocoileus hemionus*), for which infection is fatal (Fig. 1; see the Supplementary Materials for a more detailed life cycle description) (*26*). While the prevalence of *P. tenuis* infection in white-tailed deer exceeds 90% (*27*), deer populations appear to be unaffected by *P. tenuis* transmission. Consequently, high deer density is associated with high *P. tenuis* prevalence in intermediate and aberrant hosts (*26*–*28*). Furthermore, *P. tenuis* spillover from deer to moose is expected to increase in response to increasing deer density across moose range in many parts of North America, including Minnesota (*29*).

In this Minnesota system, gray wolves (*Canis lupus*) are the primary predator of deer (*30*, *31*) and moose (*25*, *32*). Deer demonstrate semimigratory behavior (*33*), and space-use changes driven by predation

[1]Veterinary Population Medicine, University of Minnesota, 1988 Fitch Ave, 495 AnSci/VetMed Bldg, St. Paul, MN 55108, USA. [2]Movement and Population Ecology Laboratory, Ecology Department, Federal University of Mato Grosso do Sul, Av. Costa e Silva, s/n°, Bairro Universitário, Campo Grande-MS 79070-900, Brazil. [3]Grand Portage Band of Lake Superior Chippewa Biology and Environment, 27 Store Road, Grand Portage, MN 55605, USA. [4]Department of Fisheries, Wildlife and Conservation Biology, University of Minnesota, St. Paul, MN 55108, USA. [5]Department of Fish and Wildlife Conservation, Virginia Polytechnic Institute and State University, Blacksburg, VA 24601, USA.
*Corresponding author. Email: gu_tapirus@hotmail.com

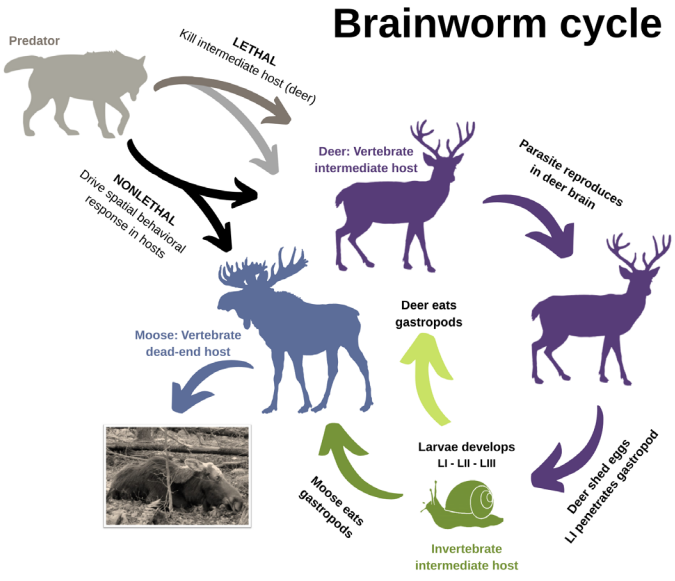

Fig. 1. Hypothesized predator impact on *P. tenuis* transmission cycle between white-tailed deer (*O. virginianus*) and moose (*A. alces*). The parasite *P. tenuis* replicates within the white-tailed deer, the definitive vertebrate host (purple). Deer shed the parasite's first-stage larvae through feces, which then infect terrestrial gastropods (snails and slugs) to develop to third-stage larvae (green). Infectious gastropods are incidentally consumed by white-tailed deer (light green arrow), in which the life cycle continues with further development to the adult stage and reproduction, or moose (green arrow), where infections are fatal and the parasite is unable to complete its life cycle (blue arrow). Wolves (gray) are hypothesized to trigger lethal and nonlethal cascade effects that influence parasite transmission from deer to moose. For example, deer are a primary prey species of wolves in Minnesota; thus, predation modulates deer density, which would consequently reduce *P. tenuis* shedding into the environment (dark gray arrow). Wolves also remove *P. tenuis*–infected, sick moose from the system, although this would not be expected to affect transmission because moose are an aberrant host [light gray arrow; (*25*, *26*)]. We postulated and tested in this study the existence of nonlethal mechanisms (black arrows), such as behavioral responses by prey to predator presence, that influence habitat use and prey species overlap, where a reduction in the latter would reduce risk of parasite transmission between prey species. Inset: Moose exhibiting *P. tenuis*–induced neurological signs (*80*).

risk might be expected in both cervid species (*30*, *34*). This offers an opportunity to understand how predators (wolves) may drive seasonal changes in space use by the definitive (deer) and aberrant hosts (moose) in a heterogeneous landscape. We hypothesized that predator-driven space use changes may produce spatial compartmentalization or segregation, which could alter spillover risk to the aberrant host through a nonlethal cascade effect.

We used 10 years of GPS-telemetry data from sympatric deer, moose, and wolves coupled to satellite-derived habitat data to investigate how predation risk influences *P. tenuis* spillover. Our goal was to describe the nonlethal-predator effect on the timing, direction, and magnitude of host movement that contributes to the spatial compartmentalization of cervid hosts on the Grand Portage Indian Reservation in northeastern Minnesota, where moose and deer serve as important subsistence species for the indigenous nation. Our specific aims were to (i) characterize the effects of season and predation risk on host habitat selection, (ii) identify the spatial overlap of deer and moose hosts as a surrogate of spillover risk, and (iii) quantify host compartmentalization through seasons and under different levels of predation risk.

RESULTS

We captured and tracked 94 adult moose, 89 deer (65 adults), and 47 adult wolves during the 2007–2019 study period, yielding about 2 million movement locations. We tracked individuals for an average of 22.9 months (range, 5.6 to 100) for moose, 10.7 months (range, 1.8 to 36.7) for deer, and 7.3 months (range, 3.4 to 21.4) for wolves. Because of strong environmental seasonality in our study area, some moose and deer migrate, which we expected to affect parasite transmission. Therefore, we used parametric net squared displacement (NSD) to characterize the movement pattern of study subjects that we tracked for at least 9 months and quantified the proportion of each population performing different movement syndromes: nomadic, sedentary, dispersal, and migratory (fig. S1). We classified 54 (83%; $n = 65$) moose and 33 (80%, $n = 41$) deer as dispersers or migrators.

Seasonality is critical to understanding *P. tenuis* epidemiology because of evidence of (i) seasonal survivorship of larvae, (ii) seasonal availability of intermediate vectors (snail and slugs), and (iii) seasonal brainworm-induced moose mortality (see *P. tenuis* life cycle in the Supplementary Materials). Standard season classification relies on a fragile assumption of climate homogeneity across years and response homogeneity among individuals, which could be unrealistic for most populations and problematic for those composed of semi-migratory individuals living in an area experiencing rapid climate change. Conversely, a classification using migratory and dispersing individuals rigorously informs what should be considered seasons for our populations (see the "Movement syndrome classification by individual" section in Materials and Methods). Thus, we used the estimated parameters for the migratory and dispersal NSD equations to estimate season dates: winter, summer, and migration dates. Migration generally occurred between March and April (i.e., spring migration) and again between October and November (i.e., fall migration) for deer and moose (fig. S1). Deer migrated farther (mean = 18.8 km, 3 to 92 km), typically in a north-south direction, than moose (mean = 5.3 km, 1.4 to 26 km) that favored a west-east direction (Fig. 2 and fig. S1).

Mapping predation risk

To model associations between predation risk and prey habitat selection, we first created a predation risk surface that captured variation in time spent by wolves (weighted by pack size) across the study site. We estimated the mean number of individuals in each pack based on direct observations from aerial tracking flights. A network cluster analysis of collared wolf locations consistently identified five packs inhabiting the study area (fig. S2). Validation using aerial monitoring records also revealed that our cluster analysis appropriately classified all wolf individuals ($n = 15$) in the correct pack, confirming the validity of a network-modeling approach to estimate pack number, distribution, and composition. Individuals tracked for multiple seasons or years demonstrated home range stability (i.e., area overlap between seasons and years) of >77 and >86%, respectively. We estimated pack home range based on standard kernel density and then used the packs' kernel utilization distribution, weighted by pack size, to build a continuous surface representing spatial variation in predation risk. Individual movement and predation risk data supported our three main assumptions: (i) individuals demonstrated pack fidelity and (ii) pack territories were stable between seasons and (iii) among years.

Habitat selection

We investigated habitat selection of migrating and dispersing deer and moose using step selection functions (SSFs) (*35*). The top-ranked

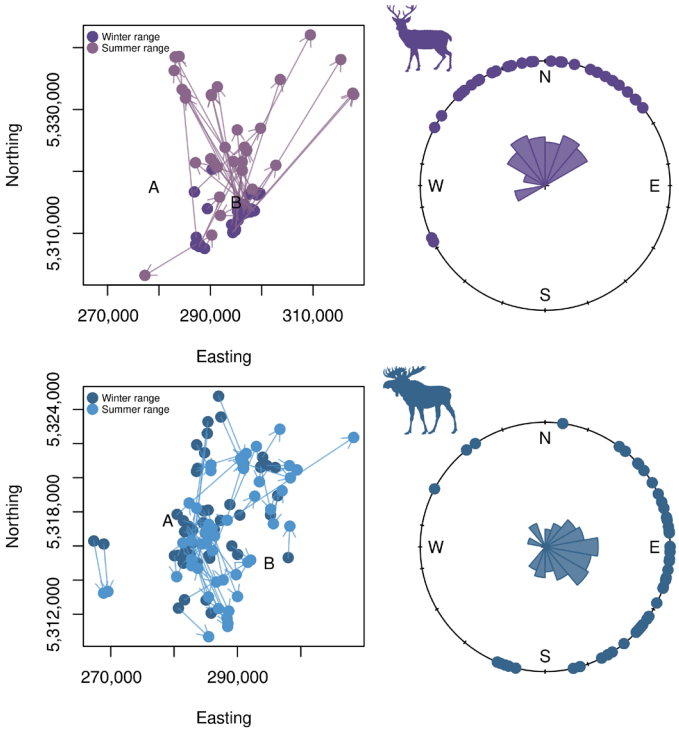

Fig. 2. Migratory movements of moose (*A. alces*) and white-tailed deer (*O. virginianus*), Grand Portage Indian Reservation, northeastern Minnesota. Left: Estimated centroid of winter and summer range for each individual vertebrate host (deer and moose). Centroids were calculated by averaging easting and northing coordinates after trajectory splitting in summer, spring migration, and winter locations. Right: Circular histogram of migration directions.

model for both deer and moose was the full SSF model that included habitat (with covertype and elevation as proxies), predation risk, and their interactions with season (table S1, $w \sim 1$). Other simpler models received less support (table S1; ΔAIC > 25 and $w \sim 0$). Both season and wolf predation risk modulated habitat selection of deer and moose (i.e., covertype and elevation; table S2). The second-best models suggested that changes in habitat selection were driven more by season for moose and by predation risk for deer (table S1). We observed differences between deer and moose in the association of habitat selection and predation risk (Fig. 3 and table S2).

The best deer and moose SSF models, which included all variables (i.e., predation risk, season, covertype, and elevation) and their interactions, were assessed under two specific wolf predation risk scenarios: average and minimum risk. Model outputs revealed that under average wolf predation risk during winter, deer and moose exhibited similar resource selection, except for elevation (Fig. 3 and table S2; coniferous forest was set as reference class). During winter, deer and moose selected mixed and deciduous forest, avoided wetlands, urban areas, and water bodies, and used open areas according to its availability (Fig. 3C); however, moose selected highlands, while deer selected lowlands (Fig. 3C). During spring migration, deer and moose selected open areas but switched elevation. That is, deer moved to high elevations and moose moved to low elevations (Fig. 3B). In summer, deer were generalists, moving through covertypes and elevations according to availability but continued avoiding urban areas and water bodies (Fig. 3A). In contrast, moose strongly selected open areas, wetlands, and mixed and deciduous forests, with low selection for coniferous forests, and indiscriminate selection of elevation.

Under minimum wolf predation risk during winter, deer selected only coniferous forests (the reference class), used deciduous forest according to availability, and further selected lower elevations (Fig. 3F). Moose showed small increases in selection for open areas and highlands (Fig. 3F). In general, the observed selection of covertypes in winter persisted during spring migration and summer, except for elevation (Fig. 3, D to F). During migration and summer seasons under minimum wolf predation risk, both deer (which selected highlands under average risk) and moose (which selected lowlands under average risk) moved irrespective of elevation (Fig. 3, A, B, D, and E). This result revealed differentially selected habitats by hosts in association with predation risk.

Compartmentalization and *P. tenuis* risk

The overall parasite spillover risk from deer to moose was characterized by tractable and predictable effects of predation risk on the spatial and temporal overlap of the two prey species. Accounting for availability of specific habitat types in the landscapes occupied by prey showed differences in the selection of rare habitats between prey species. For example, rare but highly selected habitats played little role in the overall prey overlap, while regularly distributed, common habitats contributed substantially to prey overlap. Parasite spillover risk was summarized in each season based on extent (RO50%) and overlap indices [*D*, *I*, and rank correlation (*r*)] between deer and moose hosts (*36*), in which RO50% depicts the area of overlap between the core distribution for each species, while indices (*D*, *I*, and *r*) measure overlap by taking into account the entire surface of each species' distribution probability (see the "Compartmentalization and spillover risk" section in Materials and Methods). Habitat suitability models, built according to habitat selection coefficients estimated in SSF, predicted moderate overall *P. tenuis* spillover risk based on deer-moose overlap (RO50% = 12 to 26%; $D = 0.54$ to 0.59; $I = 0.84$ to 0.85; $r = -0.02$ to 0.05; Figs. 4 and 5). Parasite spillover risk increased gradually from prey movement in winter (RO50% = 12%) through spring (RO50% = 16%) and to summer (RO50% = 26%). Spillover risk areas clustered at intermediate elevations, where deer and moose shifted from their divergent winter selection patterns during migration and summer (Figs. 4 and 5).

To validate the parasite spillover model, we necropsied 29 moose from the study area to test whether moose that died with *P. tenuis* infection used habitat with higher *P. tenuis* risk. Because our spillover risk map was a continuous heterogeneous surface of risk values and individual moose can (and did) move through areas of high and low risk, we overlaid the trajectories of each necropsied moose onto the risk map and averaged the risk values for the areas used by each moose. Thus, each necropsied moose received a value that captured the *P. tenuis* spillover risk for the area where it lived. Last, we compared these risk values between moose that died with *P. tenuis* and moose that died from other causes. *P. tenuis* infection was confirmed in 21% ($n = 6$) of necropsied moose, and those confirmed with *P. tenuis* infection at mortality used areas that were 25% riskier (higher overlap with deer) than those areas used by moose that died from other causes (coefficient = 0.25, $t = 2.19$, $P < 0.03$; fig. S3). These findings demonstrate that our spillover risk model, which accounts for prey movement in association with predator pressure, was able to predict parasite spillover better than by chance.

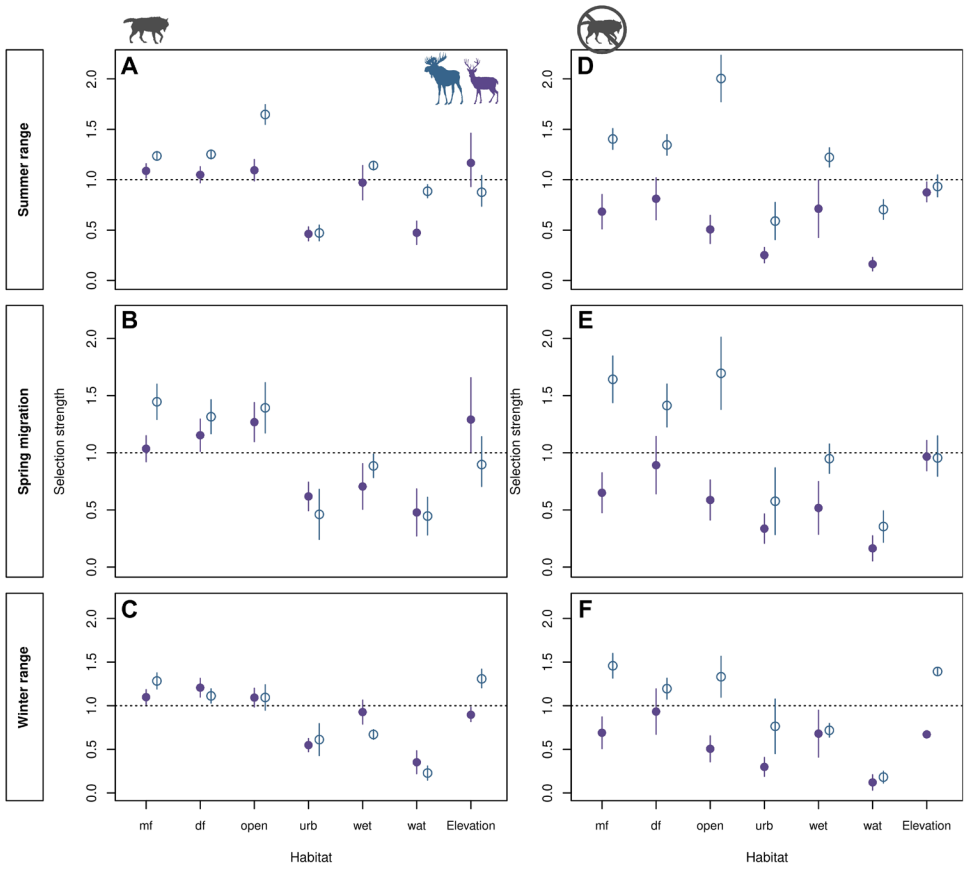

Fig. 3. Prediction of selection strength of vertebrate hosts [white-tailed deer (*O. virginianus*, purple) and moose (*A. alces*, blue)] for covertypes and elevation across seasons under two scenarios of predation risk. Expected selection strength under average wolf predation risk in summer range (**A**), spring migration (**B**), and winter range (**C**). Expected selection strength under minimum wolf predation risk in summer range (**D**), spring migration (**E**), and winter range (**F**). Predictions for average and minimum wolf predation risk scenarios were made by fixing the wolf predation risk covariate to the average and the minimum observed across space, respectively. Selection strength (between 0 and ∞+) depicts the relative risk (odds ratio) of a moving individual to choose a given habitat, conditional on its local availability. Values above dashed line indicate that covertype was selected, while those below the dashed line indicate an avoided covertype. Open circles represent estimates for moose, and closed dots represent deer estimates. Whiskers depict 95% confidence interval of estimates. Land-cover type abbreviations: mf, mixed forest; df, deciduous forest; open, open areas; wet, wetlands; wat, water bodies; urb, urban areas.

Following model validation, we further explored how predator pressure might influence the overall spatial overlap between hosts and, consequently, *P. tenuis* spillover risk to moose by modeling the latter under low predation risk. Low levels of predation risk by wolves increased *P. tenuis* spillover risk by 1.01 to 1.81 times, mainly during migration and summer ranges [RO50% = 29% (1.81 times) and 39% (1.50 times), respectively; Figs. 4 and 5]. Low predation risk by wolves increased the overlap between deer and moose from slightly (D = 1.03 to 1.05 times; I = 1.01 to 1.03 times) to strongly (r = 2.15 to 5.08 times) depending on the index used. In other words, the presence of predators reduced host species overlap between deer and moose, decreasing the likelihood of disease emergence in a vulnerable wildlife population (i.e., moose).

DISCUSSION

Ecological theories predict that predators modulate parasite transmission risk by decreasing contact rates between hosts (*8*, *10*). In this system of parasite spillover between prey species, we hypothesized that lower contact rates among prey were related to nonlethal cascade effects triggered by predator presence, limiting parasite transmission to the aberrant host. Here, we describe a nonlethal mechanism of predator-induced cascade effect on parasite transmission among prey through spatial segregation. We show that under higher predation pressure by wolves, moose and deer have less habitat overlap, thus potentially reducing parasite transmission risk. Because one of the prey species in our study is an aberrant host of *P. tenuis*, the nonlethal cascade effect provided survival benefits. This nonlethal predator effect could be interpreted as a potential compensatory mechanism that keeps aberrant host populations stable, in which increases of predation-induced mortality can be compensated or surpassed by decreases in disease-induced mortality (*9*).

Spatial compartmentalization in our study was mainly driven by contrasting host habitat selection under wolf predation pressure. Elevational heterogeneity was a key landscape element influencing spatial compartmentalization. Deer and moose shifted habitat selection in response to wolf pressure, becoming more similar in covertype but different in elevation. The differences in selection were primarily a result of selection changes by deer. Changes in habitat selection driven by wolf presence have been reported for several

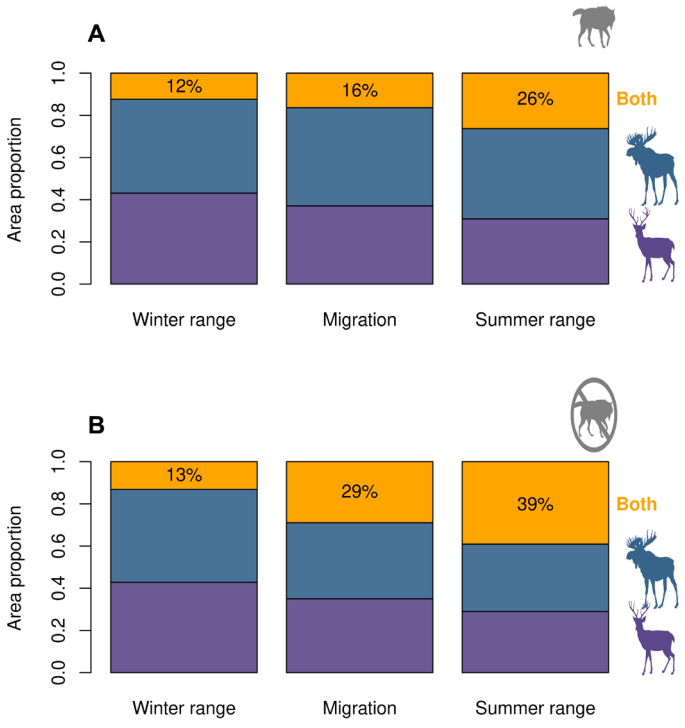

Fig. 4. Summary of spillover risk (RO50%) observed in the HSMs through time under two scenarios of wolf predation risk. Proportion of overlap (spillover risk) and exclusive areas for deer and moose during winter range, migration, and summer range under average predation risk (**A**) and under minimum wolf predation risk (**B**). Purple, blue, and orange bars indicate deer exclusive area, moose exclusive area, and overlap area of deer and moose, respectively.

prey species such as elk (*7*, *37*), caribou (*38*), white-tailed deer (*39*), and moose (*40*, *41*) and are also consistently observed as elevational shifts (*37*). We found that predator-associated changes in selection for elevation by deer were more evident during summer, consistent with previous reports (*37*). Such selection has been suggested as a predator escape strategy via flight (*42*). During winter, when snow impedes escape, antipredator behavioral strategies have been displayed, such as grouping (*43*). The fact that deer responded strongly to predator presence with altered habitat selection could be explained by the higher importance of deer than moose in the diet of wolves in this system (*44*, *45*). Changes in moose habitat selection were associated more with season than predation and followed the general temporal expectation of covertype selection for this species [i.e., mixed forest in winter and wetlands/open areas in summer; (*46*)]. Although predator presence can affect how prey use different covertypes (*7*) and elevation (*37*), we found stronger shifts of prey by elevational distribution.

Migration is a strategy many species have evolved to maximize fitness in seasonal environments (*47*) and can provide benefits to a species through escape from parasites (*48*) or confer costs via exposure to new parasites (*49*). In our parasite spillover system, spring migration and settlement in summer were detrimental for moose due to the increased spatial overlap with infected deer (*29*) at a time when *P. tenuis* shedding by deer is greatest and invertebrate intermediate hosts are available for parasite transmission (*26*). Therefore, the nonlethal effect of wolves gains relevance during these crucial seasons as the spatial compartmentalization associated with wolf presence reduced *P. tenuis* spillover risk.

Our *P. tenuis* risk estimates were guided by spatial and temporal overlap between infected and susceptible cervid hosts. We assumed, on the basis of previous studies (*27*), that infection among deer was high; thus, any overlap with deer in space presented a risk to aberrant hosts. There are factors that influence survival of larvae and intermediate hosts, which were not considered in our models. For example, weather patterns, such as the absence of snow, milder temperatures, and increased precipitation, favor first-stage larvae survival on deer feces and in leaf litter, as well as the abundance, activity, and survival of invertebrate hosts (*26*, *50*). Shaded, wet habitats are similarly favorable for larvae and invertebrate hosts. Parasite prevalence in gastropods has been found to be six times higher in forested, wet habitats than in dry upland forest (*51*), although conflicting evidence has demonstrated swamp conifer forest with the lowest gastropod abundance among covertypes (*50*) and upland conifer forest and upland shrub with higher parasite prevalence in gastropods than lowland coniferous or deciduous forest [(*52*); see the "*Parelaphostrongylus tenuis* life cycle" section in Extended methods in the Supplementary Materials]. Future studies should aim to include levels of invertebrate intermediate hosts (i.e., terrestrial gastropods) at the cost of model complexity. Given the heterogeneity in gastropod abundance and *P. tenuis* prevalence rates across habitats (*50*–*53*), we expect that risk estimates accounting for the intermediate host may add greater specificity to forecasts. We neglected intermediate hosts in our models due to data limitations and because deer density combined with high rates of infection directly influences parasite prevalence among intermediate hosts (*26*, *54*).

The overall impact of wolves on prey behavior (i.e., landscape of fear) is an open, exciting field of investigation in wildlife epidemiology. Beyond the alleviation of parasite transmission provided by wolves to moose described here, wolves are also the main predator of deer, the parasite reservoir. Thus, the suppression of deer density by wolf predation could provide further benefits to vulnerable moose by decreasing density-dependent parasite transmission from deer (*26*), as well as ecological competition release of moose (*55*, *56*). On the other hand, wolves are also a primary predator of moose calves (*32*, *57*). Summarizing these direct and indirect effects of predators in multihost parasite systems is a cornerstone step toward a better understanding of the ecology of spillover, as well as of the importance of top predators to modulate disease emergence in naïve host species (*9*). From a practical perspective, application of our discoveries could inform and improve ongoing deer management actions for disease control (e.g., chronic wasting disease, *Fascioloides magna*, and *P. tenuis*), such as broad-scale deer culling and increased deer hunting opportunities (*58*). Our findings also call for an adaptive management approach that not only examines the impact of wolf predation on moose calf survival but also considers the cascading disease transmission implications of wolves in the broader system due to their impact on deer density, habitat selection responses of cervid prey species, and *P. tenuis* incidence in moose.

This study demonstrates how incorporating predator occurrence, host movement, and habitat heterogeneity can reveal the spatial profile of parasite spillover in prey. We uncovered a previously unrecognized spatial compartmentalization effect of predators on parasite spillover risk, manifested indirectly through nonlethal cascade effects. These findings are particularly relevant to disease ecology studies in wildlife hosts.

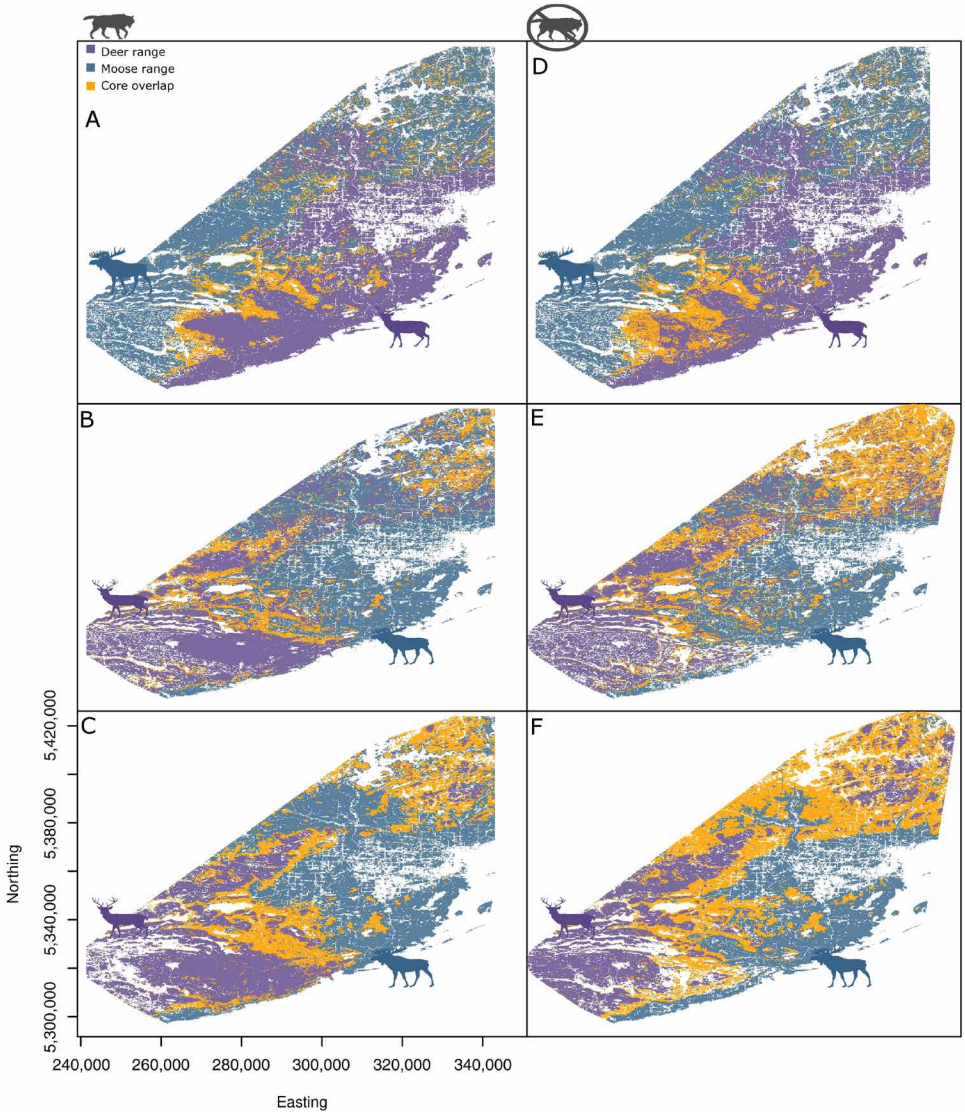

Fig. 5. HSM of vertebrate hosts [white-tailed deer (*O. virginianus*) and moose (*A. alces*)] under two scenarios of predation risk. HSM in winter range, spring migration, and summer range from top to bottom, respectively. Left: HSM when predation risk was set as the observed values: winter range (**A**), spring migration (**B**), and summer range (**C**). Right: HSM when predation risk was set as the observed minimum: winter range (**D**), spring migration (**E**), and summer range (**F**). Purple polygons indicate HSM for white-tailed deer, blue polygons indicate HSM for moose, and orange polygons indicate the core range overlap (RO50%) between moose and deer HSMs. Continuous probability surfaces were categorized according to the isopleth of 50% of the distribution probability from each species (core range). Note that this pattern was based on disperser and migrator individuals that represent over 80% of tracked individuals.

MATERIALS AND METHODS

Study area and species

We conducted this study in and around the Grand Portage Band of Lake Superior Chippewa Indian Reservation in northeastern Minnesota, United States, in the northern superior uplands forest region along the northwest Lake Superior shoreline (4°50′N, 92°8′W). The reservation (227 km^2) is bordered to the north by the Pigeon River and Ontario, Canada; to the southeast by 39 km of Lake Superior shoreline; and to the west by a mix of federal, state, and private lands. The landscape was characterized by a matrix of forested stands and wetlands, dominated by conifer, deciduous, and mixed conifer-deciduous forests (*59*). In this study area, moose co-occurred with deer, and both were primarily preyed upon by gray wolves (*25*, *31*, *32*). Moose density was approximately 0.26 individuals/km^2 [90% confidence interval, 0.21 to 0.34] (*24*), deer density was 0.76 to 3.80 individuals/km^2 (*60*), and wolf density was approximately 0.03 individuals/km^2 (*61*). The parasite *P. tenuis* occurred naturally in deer, where minimum to nil negative effects are observed, while accidental infections in naïve species, such as moose, are fatal. More details of the study site and the *P. tenuis* life cycle are available in the Supplementary Materials (Extended methods).

Animal capture, handling, and tracking

Captures of wolves, moose, and deer were part of long-term research led the by the Grand Portage Band. We captured moose and deer January to March from 2010 to 2019 by netgunning or aerial darting

from helicopter (for moose) or corn-baited Clover traps (for deer). We captured wolves throughout June to November from 2007 to 2019 using foothold traps. Moose were chemically immobilized using either carfentanil citrate (4.5 mg), etorphine hydrochloride (8.5 to 10 mg), or thiafentanil oxalate (10 mg) combined with xylazine (40 to 50 mg). Before removal from traps, deer were chemically immobilized with ketamine hydrochloride (3.5 to 7.5 mg/kg) and xylazine (1 to 3 mg/kg) and wolves with ketamine (7.5 mg/kg) and xylazine (1.5 mg/kg). We fitted captured individuals with a GPS collar programmed to record geographical locations and timestamps every 2 to 4 hours and equipped with a movement-based mortality sensor, communicating a mortality event via satellite transmission when movement diminished below a programmed threshold after a period of 6 hours. We tracked collared moose until mortality or collar failure, confirming cause of death based on a comprehensive site investigation and necropsy/histopathologic examination. When possible, we extracted and transported the full carcass to the University of Minnesota Veterinary Diagnostic Laboratory (MNVDL) (St. Paul, MN) for complete necropsy, histopathology, and disease screening. Otherwise, we performed a field necropsy and submitted a representative set of tissue samples to the MNVDL for histopathology. We characterized a moose as infected with *P. tenuis* (case) if we detected the nematode and/or lesions caused by its migration tract in neural tissues, combined with lymphoplasmacytic encephalitis, leptomeningitis with plexus coroiditis, gliosis, and/or focal axonal spheroid formation (*62*). If we did not observe postmortem lesions, we considered the individual to be negative (control) for *P. tenuis* for further analyses. All capture and handling protocols were conducted in accordance with requirements of the University of Minnesota Institutional Animal Care and Use Committee (protocols 1410-31945A, 1601-33318A, 1812-36635A, and 1803-35736A).

Habitat covariates

We classified the landscape into broad land-cover type classes (hereafter covertypes) and continuous values of landscape elevation. We used two open-source land-cover classifications available for the United States (National Land Cover Database, NLCD 2011) and Canada (Land Cover of Canada, LCC 2015). We aggregated original cover types into six classes (table S3): water bodies, wetlands, coniferous forest, deciduous forest, mixed forest, and urban/developed areas. We accessed elevation using the digital elevation model generated by Shuttle Radar Topography Mission (NASA-STRM) at 30-m horizontal resolution and 1-m vertical resolution, available for downloading in R using the elevatr package (*63*).

Mapping predation risk

We represented the continuous spatial variation in predation risk perception for deer and moose throughout the wolf territories by pack-based utilization densities, each weighted by pack size. First, we estimated the home range for each individual wolf by calculating the 95% isopleth (kernel 95%) of each animal's utilization distribution (based on kernel density estimation) (*64*). We use the "h of reference" calculation to estimate the smoothing parameter used to build the two-dimensional Gaussian kernel function. We then calculated a matrix of pairwise home range overlap values among individuals based on Bhattacharyya's affinity method (*65*). This method is a symmetric index (i.e., only one value for each pair of individuals) that calculates the similarity between the utilization distributions of two individuals. The index ranges from 0 (no overlap) to 1 (perfect overlap) and takes into account the entire kernel density surface. We used a social network approach over the home range overlap matrix to estimate the number of packs and their individual composition. We built an undirected, weighted social network, in which individuals were vertices and the edges (degree of association among individuals) were depicted by the magnitude of overlap (*66*). We estimated the pack number and composition with a cluster algorithm that detects group structures within networks (*67*). This algorithm initialized with a unique group label for each vertex (individual), and at every iterative step, each vertex received the group label that most of its neighbors (individuals with high overlap) had. This process ran until densely connected individuals formed a consensus on a unique label group to form a pack. Before cluster processing, we removed edge values less than the median edge value.

Once we identified pack number and composition, we estimated the pack utilization distribution by summing the utilization distributions of each home range within each pack. We rescaled each pack utilization distribution [0 (lowest density) to 1 (highest density)] and multiplied by its mean number of individuals. We estimated the mean number of individuals in each pack based on direct observations from aerial tracking flights. Last, we summed pack utilization distributions (rescaled and multiplied) as a proxy of the overall spatial distribution of predation risk across the entire study area [sensu (*7*)]. We set the spatial distribution of predation risk as a raster with the same extent and resolution of the covertypes and elevation rasters. We also recorded collared wolves observed together (i.e., those belonging to the same pack). These records allowed us to validate the precision of our network cluster classification. We performed home range estimations using the adehabitatHR package (*68*), network building, handling, and clustering with the igraph package (*69*), and algebra of utilization distribution raster with the raster package (*70*) in R.

Movement syndrome classification by individual

We used a parametric NSD approach to classify individual deer and moose into four movement syndromes: nomadic, sedentary, dispersal, and migratory (*71*). The mean NSD is the linear distance between the initial location (starting point) and successive locations of a moving particle through time (*71*). The functional shape of NSD through time for each syndrome has specific theoretical expectations and can be captured through nonlinear models [see details in (*71*)]. Briefly, in Eq. 1, the NSD curve for nomadic trajectories (Brownian motion or diffusive regime) would increase linearly with time *t*. Accordingly

$$\mathrm{NSD} = 4 * Dt \tag{1}$$

where *D* is a diffusion constant. A sedentary trajectory is constrained by boundaries (i.e., home range) and NSD would initially increase linearly, but the increasing rate should decrease (subdiffusive) over time *t* until it reaches an asymptotic value

$$\mathrm{NSD} = 3 * D^2/c^2 \tag{2}$$

where *c* is an advection coefficient that quantifies the attraction strength to the starting point (home range center). A dispersal particle presents two stationary phases (departure and settlement) separated by a transient phase. Thus, the NSD curve would have a

sigmoidal shape over time t with values close to zero during departure, a linear increase while transient, until it reaches a new stationary value with settlement

$$\mathrm{NSD} = \mathrm{Asym}/1 + \exp(\mathrm{tmid} - t)/\mathrm{scal} \quad (3)$$

where Asym is the asymptote of settlement, tmid is the time of inflection point at transient phase, and scal is the scale determining the transient phase velocity. A migration particle would be a combination of two dispersal events, where the second event is the return to the starting point

$$\mathrm{NSD} = \mathrm{Asym}/(1 + \exp(\mathrm{tmid}_1 - t)/\mathrm{scal}_1) + \mathrm{Asym}/(1 + \exp(\mathrm{tmid}_2 - t)/\mathrm{scal}_2) \quad (4)$$

where subscript indices (1 and 2) depict parameters associated with transient phases of dispersal and return, respectively [see (*68*)].

We fit these models (Eqs. 1 to 4) for each individual using a nonlinear least-squares approach. We selected the best model (i.e., movement syndrome) for each individual based on Akaike's information criterion (AIC) (*72*). We applied the movement syndrome classification only for adult deer and moose that we tracked for at least 9 months. Because we were interested in large-scale movement patterns, we subsampled trajectories using one location per day to fit the models. We handled individual trajectories using the adehabitatLT package (*68*) and fit nonlinear models using nls.multstart packages (*73*) in R.

Seasonal movement

Rather than classify seasons based on standard, but arbitrary Julian dates [e.g., winter, spring, and summer; (*34*)], we used movement data to inform when individuals departed from one seasonal range (winter or summer) and settled in the other; this approach allowed for annual and individual variation in perception of environmental and internal cues that trigger migration events. We derived biological season dates by first defining the transient phase boundaries (*71*): from departure time in winter range ($\mathrm{dw} = \mathrm{tmid}_1 - 3{*}\mathrm{scal}_1$) until settlement in summer range ($\mathrm{ss} = \mathrm{tmid}_1 + 3{*}\mathrm{scal}_1$), and from return time in summer range ($\mathrm{ds} = \mathrm{tmid}_2 - 3{*}\mathrm{scal}_2$) to resettlement in winter range ($\mathrm{sw} = \mathrm{tmid}_2 + 3{*}\mathrm{scal}_2$). We thus split individual trajectories following individual estimated dates. We considered transient relocations (spring and autumn migration) as those that occurred between dw and ss or between ds and sw, and summer relocations as those occurring between ss and ds and winter between sw and dw.

Habitat selection

We investigated habitat selection of deer and moose using SSFs (*35*). SSF models are an improvement over standard resource selection functions, which consider that resource availability is not fixed and depends on the individual's position, as well as its movement and orientation capacity (*35*). First, we subsampled each individual trajectory to 4 hours (originally composed of 2 to 4 hours). We decomposed trajectories into two components: step length and turning angle. For each individual location (step starting point), we measured resource availability by generating 30 random steps originating from it. We generated random steps by sorting independent random samples from each individual's observed distribution of step lengths and turning angles [empirical sampling; (*74*)]. For each observed (coded as 1s) and random step (coded as 0s), we recorded the covertype (categorical), elevation (continuous), and predation risk (continuous) in which the ending point fell, as well as the season in which the step occurred (categorical: winter, summer, and the transient phase of spring migration).

We fit SSF models using unweighted mixed conditional Poisson regression (MCPR) (*75*). This mixed approach mathematically mimics the traditional conditional logistic regression approach of SSF but with fast processing time and accurate selection estimates obtained by controlling for individual heterogeneity [see details in (*75*)]. We included habitat covariates (covertypes and elevation), season, and predation risk as fixed effects, and individual identity as a random intercept to account for individual heterogeneity in resource selection. We chose coniferous forest as the reference covertype. We also included interaction terms between the habitat covariates and season, and habitat covariates and predation risk, which permitted testing if selection strength for a given resource changed depending on season or predation risk. We conditioned MCPR to each step by also including step identity as a random intercept, ensuring that each observed step (used) was compared with its respective surrounding availability. However, we did not estimate the variance of the random intercept for steps but instead fixed it to "infinite" (10^6) to avoid sub-estimation of SEs associated with fixed effects, as recommended by (*75*). We z-standardized continuous covariates before fitting the SSF model to allow comparisons among estimated coefficients.

We fitted four SSF models for moose and deer, separately. We built models in increasing order of complexity: (i) habitat model, which included habitat covariates: covertype and elevation; (ii) dynamic habitat model, which included covertype, elevation, and their interaction with season; (iii) habitat-predator model, which included habitat covariates and predation risk; and (iv) full model, which included habitat and predator covariates, as well their interactions with season. We ranked these models for each species using AIC. If more than one model within a species were equally plausible ($\Delta\mathrm{AIC} < 4$) (*72*), we averaged the estimated coefficients to draw conclusions. This approach allowed testing of concurrent models about how these two species perceive the landscape and what factors are most important to individuals' spatial distribution. We only included disperser/migrator adult individuals with more than 9 months of tracking within a year in SSF analyses. The effects of wolf predation risk on deer and moose habitat selection were assessed using the best-ranked SSF model for each species. We used these models to make predictions under two predation risk scenarios: average and minimum. For the average risk scenario, we made predictions setting the predation risk covariate to the average of the observed values of predation risk, while for the minimum risk scenario, we set it to the minimum observed. These two risk levels were selected because they represented two realistic extremes [observed wolf pressure and minimum wolf pressure (e.g., a sharp drop in wolf population)]. Maximum wolf predation risk was not a reasonable consideration because the wolf population at the study site is healthy, and it is unlikely to increase much in the near future. On the other hand, wolf management is changing and threats are present, so this predator population may decline, as has been observed throughout its distributional range. We handled trajectories using the amt package (*76*) and fit MCPR models using the glmmTMB package (*77*) in R.

Compartmentalization and spillover risk

The underlying assumption of our spillover risk map is that places with high overlap between moose and deer are risky areas for

P. tenuis spillover to moose. Estimated coefficients of SSF models have been used to inform habitat suitability models (HSMs) or species distribution models [e.g., (*78*)]. Therefore, we used the estimated coefficients of the best-ranked models for moose and deer to predict an HSM for both species across the entire study area in each season. We used the best-ranked SSF model of both species to predict selection strength for each raster cell. We rescaled the predicted values in raster cells between 0 (low suitability) and 1 (high suitability) and then multiplied the HSM of deer and moose (i.e., overlapped) to obtain a map of *P. tenuis* risk. We summarized the degree of spatial overlap in each season by calculating the range overlap for isopleth of 50% (RO50%) and the niche overlap (*D*, *I*, and *r*) between HSMs [sensu (*36*)]. Range overlap and *D* and *I* indices vary from 0 (no overlap) to 1 (perfect overlap between HSM areas), while *r* index varies from −1 (opposite correlation between probability of distribution) to 1 (positive correlation). These indices of overlap represent proxies for the degree of compartmentalization between species, in which higher values indicate compartmentalization by packing (high risk), while lower values indicate compartmentalization by segregation (low risk). While RO50% estimates the area of overlap between the core areas of distribution for each species, the indices measure the overlap taking into account the entire surface of the distribution probability for each species. Specifically, *D* (Schoener's statistic) and *I* (Hellinger-based distance) sum up the absolute and the squared differences in standardized probability between pairs of pixels, respectively. We graphically represented the proposed risk map highlighting the overlapped areas retained in the RO50%. We manipulated rasters and spatial prediction with SSF model output using the raster package in R.

We validated the risk map using movement data from collared moose that died with *P. tenuis* infection versus those that died of other causes [e.g., wolf predation and winter tick (*Dermacentor albipictus*) infestation and other nonpredation health issues], where *P. tenuis* infection was not detected. For confirmed cases of *P. tenuis* mortality, we extracted the last 180 days of tracking before death to represent the spatial range where individuals might have been exposed to *P. tenuis*, but excluded the last 60 days [expected incubation time for *P. tenuis* disease; (*79*)] of each trajectory to exclude any abnormal movement caused by *P. tenuis* infection or associated with other causes of death. Sequentially, we overlapped these trajectories over the proposed risk map and calculated the mean *P. tenuis* risk experienced by each moose (i.e., mean of the map risk values linked to relocations). Last, we compared the observed mean of *P. tenuis* risk between cases and controls using a *t* test. We expected that moose that died with *P. tenuis* infection should present higher risk values than controls, thus validating the *P. tenuis* spillover risk map.

To quantify the impact of wolf presence on the overall spatial overlap between hosts and consequently on *P. tenuis* spillover risk to moose, we reestimated deer and moose HSM's by fixing wolf predation risk values to the minimum observed. Sequentially, we recalculated the range overlap index (RO50%) and niche overlap indices (*D*, *I*, and *r* indices) and compared them with indices observed when wolf predation risk was set to observed values (i.e., $\text{index}_{\text{low-risk}}$/$\text{index}_{\text{observed-risk}}$).

SUPPLEMENTARY MATERIALS

Supplementary material for this article is available at https://science.org/doi/10.1126/sciadv.abj5944

REFERENCES AND NOTES

1. W. J. Ripple, J. A. Estes, R. L. Beschta, C. C. Wilmers, E. G. Ritchie, M. Hebblewhite, J. Berger, B. Elmhagen, M. Letnic, M. P. Nelson, O. J. Schmitz, D. W. Smith, A. D. Wallach, A. J. Wirsing, Status and ecological effects of the world's largest carnivores. *Science* **343**, 1241484 (2014).
2. D. J. McCauley, E. Hoffmann, H. S. Young, F. Micheli, Night shift: Expansion of temporal niche use following reductions in predator density. *PLOS ONE* **7**, e38871 (2012).
3. T. R. Hofmeester, P. A. Jansen, H. J. Wijnen, E. C. Coipan, M. Fonville, H. H. T. Prins, H. Sprong, S. E. Van Wieren, Cascading effects of predator activity on tick-borne disease risk. *Proc. Biol. Sci.* **284**, 20170453 (2017).
4. S. J. Gallagher, B. J. Tornabene, T. S. DeBlieux, K. M. Pochini, M. F. Chislock, Z. A. Compton, L. K. Eiler, K. M. Verble, J. T. Hoverman, Healthy but smaller herds: Predators reduce pathogen transmission in an amphibian assemblage. *J. Anim. Ecol.* **88**, 1613–1624 (2019).
5. P. A. Abrams, Adaptive responses of predators to prey and prey to predators: The failure of the arms-race analogy. *Evolution* **40**, 1229–1247 (1986).
6. S. L. Lima, Nonlethal effects in the ecology of predator-prey interactions. *Bioscience* **48**, 25–34 (1998).
7. D. Fortin, H. L. Beyer, M. S. Boyce, D. W. Smith, T. Duchesne, J. S. Mao, Wolves influence elk movements: Behavior shapes a trophic cascade in Yellowstone National Park. *Ecology* **86**, 1320–1330 (2005).
8. R. S. Ostfeld, R. D. Holt, Are predators good for your health? Evaluating evidence for top-down regulation of zoonotic disease reservoirs. *Front. Ecol. Environ.* **2**, 13–20 (2004).
9. E. Tanner, A. White, P. Acevedo, A. Balseiro, J. Marcos, C. Gortázar, Wolves contribute to disease control in a multi-host system. *Sci. Rep.* **9**, 7940 (2019).
10. T. Levi, A. M. Kilpatrick, M. Mangel, C. C. Wilmers, Deer, predators, and the emergence of Lyme disease. *Proc. Natl. Acad. Sci. U.S.A.* **109**, 10942–10947 (2012).
11. C. Packer, R. D. Holt, P. J. Hudson, K. D. Lafferty, A. P. Dobson, Keeping the herds healthy and alert: Implications of predator control for infectious disease. *Ecol. Lett.* **6**, 797–802 (2003).
12. M. Genovart, N. Negre, G. Tavecchia, A. Bistuer, L. Parpal, D. Oro, The young, the weak and the sick: Evidence of natural selection by predation. *PLOS ONE* **5**, e9774 (2010).
13. C. E. Krumm, M. M. Conner, N. T. Hobbs, D. O. Hunter, M. W. Miller, Mountain lions prey selectively on prion-infected mule deer. *Biol. Lett.* **6**, 209–211 (2010).
14. M. A. Wild, N. T. Hobbs, M. S. Graham, M. W. Miller, The role of predation in disease control: A comparison of selective and nonselective removal on prion disease dynamics in deer. *J. Wildl. Dis.* **47**, 78–93 (2011).
15. M. J. Keeling, P. Rohani, *Modeling Infectious Diseases in Humans and Animals* (Princeton Univ. Press, 2008).
16. O. Diekmann, H. Heesterbeek, T. Briton, *Mathematical Tools for Understanding Infectious Disease Dynamics* (Princeton Univ. Press, 2012).
17. M. A. Duffy, J. M. Housley, R. M. Penczykowski, C. E. Cáceres, S. R. Hall, Unhealthy herds: Indirect effects of predators enhance two drivers of disease spread. *Funct. Ecol.* **25**, 945–953 (2011).
18. S. A. Orlofske, R. C. Jadin, J. T. Hoverman, P. T. J. Johnson, Predation and disease: Understanding the effects of predators at several trophic levels on pathogen transmission. *Freshw. Biol.* **59**, 1064–1075 (2014).
19. R. S. Ostfeld, G. E. Glass, F. Keesing, Spatial epidemiology: An emerging (or re-emerging) discipline. *Trends Ecol. Evol.* **20**, 328–336 (2005).
20. J. A. Merkle, P. C. Cross, B. M. Scurlock, E. K. Cole, A. B. Courtemanch, S. R. Dewey, M. J. Kauffman, Linking spring phenology with mechanistic models of host movement to predict disease transmission risk. *J. Appl. Ecol.* **55**, 810–819 (2018).
21. J. A. Benavides, W. Valderrama, D. G. Streicker, Spatial expansions and travelling waves of rabies in vampire bats. *Proc. Biol. Sci.* **283**, 20160328 (2016).
22. S. Riley, Large-scale spatial-transmission models of infectious disease. *Science* **316**, 1298–1301 (2007).
23. M. W. Lankester, Extrapulmonary lungworms of cervids, in *Parasitic Diseases of Wild Mammals*, W. M. Samuel, M. J. Pybus, A. A. Kocan, Eds. (Iowa State Univ. Press, ed. 2, 2008), pp. 228–278.
24. G. D. DelGiudice, "*2019 Aerial Moose Survey*" (Minnesota Department of Natural Resources, 2019).
25. M. Carstensen, E. C. Hildebrand, D. Plattner, M. Dexter, A. Wünschmann, A. Armien, "Causes of non-hunting mortality of adult moose in Minnesota, 2013–2017" (Minnesota Department of Natural Resources, 2018).
26. M. W. Lankester, Understanding the impact of meningeal worm, *Parelaphostrongylus tenuis*, on moose populations. *Alces* **46**, 53–70 (2010).
27. A. M. Slomke, M. W. Lankester, W. J. Peterson, Infrapopulation dynamics of *Parelaphostrongylus tenuis* in white-tailed deer. *J. Wildl. Dis.* **31**, 125–135 (1995).
28. M. W. Lankester, Considering weather-enhanced transmission of meningeal worm, *Parelaphostrongylus tenuis*, and moose declines. *Alces* **54**, 1–13 (2018).

29. K. L. Dawe, S. Boutin, Climate change is the primary driver of white-tailed deer (*Odocoileus virginianus*) range expansion at the northern extent of its range; land use is secondary. *Ecol. Evol.* **6**, 6435–6451 (2016).
30. M. E. Nelson, L. D. Mech, Deer social organization and wolf *Canis lupus* predation in northeastern Minnesota. *Wildl. Monogr.* **77**, 3–53 (1981).
31. G. D. DelGiudice, M. R. Riggs, P. Joly, W. Pan, Winter severity, survival, and cause-specific mortality of female white-tailed deer in north-central Minnesota. *J. Wildl. Manage.* **66**, 698 (2002).
32. W. J. Severud, T. R. Obermoller, G. D. DelGiudice, J. R. Fieberg, Survival and cause-specific mortality of moose calves in northeastern Minnesota. *J. Wildl. Manage.* **83**, 1131–1142 (2019).
33. J. Fieberg, D. W. Kuehn, G. D. DelGiudice, Understanding variation in autumn migration of northern white-tailed deer by long-term study. *J. Mammal.* **89**, 1529–1539 (2008).
34. M. A. Ditmer, A. M. McGraw, L. Cornicelli, J. D. Forester, P. J. Mahoney, R. A. Moen, S. P. Stapleton, V. St-Louis, K. Vanderwaal, M. Carstensen, Using movement ecology to investigate meningeal worm risk in moose, *Alces alces*. *J. Mammal.* **101**, 589–603 (2020).
35. J. D. Forester, H. K. Im, P. J. Rathouz, Accounting for animal movement in estimation of resource selection functions: Sampling and data analysis. *Ecology* **90**, 3554–3565 (2009).
36. D. L. Warren, L. J. Beaumont, R. Dinnage, J. B. Baumgartner, New methods for measuring ENM breadth and overlap in environmental space. *Ecography* **42**, 444–446 (2019).
37. J. S. Mao, M. S. Boyce, D. W. Smith, F. J. Singer, D. J. Vales, J. M. Vore, E. H. Merrill, Habitat selection by elk before and after wolf reintroduction in Yellowstone National Park. *J. Wildl. Manage.* **69**, 1691–1707 (2005).
38. N. J. DeCesare, M. Hebblewhite, M. Bradley, D. Hervieux, L. Neufeld, M. Musiani, Linking habitat selection and predation risk to spatial variation in survival. *J. Anim. Ecol.* **83**, 343–352 (2014).
39. A. Massé, S. D. Côté, Habitat selection of a large herbivore at high density and without predation: Trade-off between forage and cover? *J. Mammal.* **90**, 961–970 (2009).
40. M. A. Ditmer, J. R. Fieberg, R. A. Moen, S. K. Windels, S. P. Stapleton, T. R. Harris, Moose movement rates are altered by wolf presence in two ecosystems. *Ecol. Evol.* **8**, 9017–9033 (2018).
41. M. T. Kohl, D. R. Stahler, M. C. Metz, J. D. Forester, M. J. Kauffman, N. Varley, P. J. White, D. W. Smith, D. R. MacNulty, Diel predator activity drives a dynamic landscape of fear. *Ecol. Monogr.* **88**, 638–652 (2018).
42. V. Geist, in *North American Elk: Ecology and Management*, D. E. Toweill, J. W. Thomas, Eds. (Smithsonian Institution Press, 2002), pp. 389–434.
43. M. Hebblewhite, D. H. Pletscher, Effects of elk group size on predation by wolves. *Can. J. Zool.* **80**, 800–809 (2002).
44. S. H. Fritts, L. D. Mech, Dynamics, movements and feeding ecology of a newly protected wolf population in northwestern Minnesota. *Wildl. Monogr.* **80**, 3–79 (1981).
45. T. D. Gable, S. K. Windels, J. G. Bruggink, S. M. Barber-Meyer, Weekly summer diet of gray wolves (*Canis lupus*) in northeastern Minnesota. *Am. Midl. Nat.* **179**, 15–27 (2018).
46. C. Dussault, J.-P. Quellet, R. Courtois, J. Huot, L. Breton, H. Jolicoeur, Linking moose habitat selection to limiting factors. *Ecography* **28**, 619–628 (2005).
47. T. Alerstam, A. Hedenström, S. Åkesson, Long-distance migration: Evolution and determinants. *Oikos* **103**, 247–260 (2003).
48. S. Altizer, R. Bartel, B. A. Han, Animal migration and infectious disease risk. *Science* **331**, 296–302 (2011).
49. J. Waldenström, S. Bensch, S. Kiboi, D. Hasselquist, U. Ottosson, Cross-species infection of blood parasites between resident and migratory songbirds in Africa. *Mol. Ecol.* **11**, 1545–1554 (2002).
50. T. Cyr, S. K. Windels, R. Moen, J. W. Warmbold, Diversity and abundance of terrestrial gastropods in Voyageurs National Park, MN: Implications for the risk of moose becoming infected with *Parelaphostrongylus tenuis*. *Alces* **50**, 121–132 (2014).
51. M. W. Lankester, R. C. Anderson, Gastropods as intermediate hosts of *Pneumostrongylus tenuis* Dougherty of white-tailed deer. *Can. J. Zool.* **46**, 373–383 (1968).
52. K. L. Vanderwaal, S. K. Windels, B. T. Olson, J. T. Vannatta, R. Moen, Landscape influence on spatial patterns of meningeal worm and liver fluke infection in white-tailed deer. *Parasitology* **142**, 706–718 (2015).
53. C. N. Johnson, J. Vanderwal, Evidence that dingoes limit abundance of a mesopredator in eastern Australian forests. *J. Appl. Ecol.* **46**, 641–646 (2009).
54. M. W. Lankester, W. J. Peterson, The possible importance of wintering yards in the transmission of *Parelaphostrongylus tenuis* to white-tailed deer and moose. *J. Wildl. Dis.* **32**, 31–38 (1996).
55. D. I. Bolnick, T. Ingram, W. E. Stutz, L. K. Snowberg, O. L. Lau, J. S. Paull, Ecological release from interspecific competition leads to decoupled changes in population and individual niche width. *Proc. Biol. Sci.* **277**, 1789–1797 (2010).
56. H. Bao, J. M. Fryxell, H. Liu, H. Dou, Y. Ma, G. Jiang, Effects of interspecific interaction-linked habitat factors on moose resource selection and environmental stress. *Sci. Rep.* **7**, 41514 (2017).
57. T. M. Wolf, Y. M. Chenaux-Ibrahim, E. J. Isaac, A. Wünschmann, S. A. Moore, Neonate health and calf mortality in a declining population of north american moose (*Alces alces americanus*). *J. Wildl. Dis.* **57**, 40–50 (2021).
58. F. D. Uehlinger, A. C. Johnston, T. K. Bollinger, C. L. Waldner, Systematic review of management strategies to control chronic wasting disease in wild deer populations in North America. *BMC Vet. Res.* **12**, 173 (2016).
59. T. Lillesand, J. Chipman, D. Nagel, H. Reese, M. Bobo, R. Goldmann, *Upper Midwest Gap Analysis Program Image Processing Protocol* (United States Geological Survey, 1998).
60. M. Grund, *Monitoring Population Trends of White-Tailed Deer in Minnesota 2014* (Minnesota Department of Natural Resources, 2014).
61. J. Erb, C. Humpal, B. Sampson, *Minnesota Wolf Population Update 2015* (Minnesota Department of Natural Resources, 2015).
62. M. W. Lankester, W. Peterson, O. Ogunremi, Diagnosing *Parelaphostrongylosis* in moose (*Alces alces*). *Alces* **43**, 49–59 (2007).
63. J. W. Hollister, A. L. Robitaille, M. W. Beck, M. Johnson, T. Shah, jhollist/elevatr: New {CRAN} Release v0.3.0 (2020); doi:10.5281/ZENODO.4282962.
64. B. J. Worton, Kernel methods for estimating the utilization distribution in home-range studies. *Ecology* **70**, 164–168 (1989).
65. J. Fieberg, C. O. Kochanny, Quantifying home-range overlap: The importance of the utilization distribution. *J. Wildl. Manage.* **69**, 1346–1359 (2005).
66. D. R. Farine, H. Whitehead, Constructing, conducting and interpreting animal social network analysis. *J. Anim. Ecol.* **84**, 1144–1163 (2015).
67. U. N. Raghavan, R. Albert, S. Kumara, Near linear time algorithm to detect community structures in large-scale networks. *Phys. Rev. E* **76**, 036106 (2007).
68. C. Calenge, The package "adehabitat" for the R software: A tool for the analysis of space and habitat use by animals. *Ecol. Model.* **197**, 516–519 (2006).
69. G. Csardi, T. Nepusz, The igraph software package for complex network research. *InterJ. Complex Syst.* **1695**, 1–9 (2006).
70. R. J. Hijmans, J. van Etten, M. Sumner, J. Cheng, D. Baston, A. Bevan, R. Bivand, L. Busetto, M. Canty, B. Fasoli, D. Forrest, A. Ghosh, D. Golicher, J. Gray, J. A. Greenberg, P. Hiemstra, K. Hingee; Institute for Mathematics Applied Geosciences, C. Karney, M. Mattiuzzi, S. Mosher, B. Naimi, J. Nowosad, E. Pebesma, O. P. Lamigueiro, E. B. Racine, B. Rowlingson, A. Shortridge, B. Venables, R. Wueest, raster: Geographic data analysis and modeling (2021); https://cran.r-project.org/package=raster.
71. N. Bunnefeld, L. Börger, B. Van Moorter, C. M. Rolandsen, H. Dettki, E. J. Solberg, G. Ericsson, A model-driven approach to quantify migration patterns: Individual, regional and yearly differences. *J. Anim. Ecol.* **80**, 466–476 (2011).
72. K. P. Burnham, D. R. Anderson, *Model Selection and Multimodel Inference: A Practical Information-Theoretic Approach* (Springer-Verlag New York, ed. 2, 2002).
73. D. Padfield, G. Matheson, nls.multstart: Robust non-linear regression using AIC scores (2020); https://cran.r-project.org/package=nls.multstart.
74. L. G. R. Oliveira-Santos, J. D. Forester, U. Piovezan, W. M. Tomas, F. A. S. Fernandez, Incorporating animal spatial memory in step selection functions. *J. Anim. Ecol.* **85**, 516–524 (2016).
75. S. Muff, J. Signer, J. Fieberg, Accounting for individual-specific variation in habitat-selection studies: Efficient estimation of mixed-effects models using Bayesian or frequentist computation. *J. Anim. Ecol.* **89**, 80–92 (2020).
76. J. Signer, J. Fieberg, T. Avgar, Animal movement tools (amt): {R} package for managing tracking data and conducting habitat selection analyses. *Ecol. Evol.* **9**, 880–890 (2019).
77. M. E. Brooks, K. Kristensen, K. J. van Benthem, A. Magnusson, C. W. Berg, A. Nielsen, H. J. Skaug, M. Mächler, B. M. Bolker, glmmTMB balances speed and flexibility among packages for zero-inflated generalized linear mixed modeling. *R J.* **9**, 378–400 (2017).
78. J. Signer, J. Fieberg, T. Avgar, Estimating utilization distributions from fitted step-selection functions. *Ecosphere.* **8**, e01771 (2017).
79. M. W. Lankester, Low-dose meningeal worm (*Parelaphostrongylus tenuis*) infections in moose (*Alces alces*). *J. Wildl. Dis.* **38**, 789–795 (2002).
80. Department of Environmental Conservation—Wildlife Health Unit, "Brain Worm"; www.dec.ny.gov/animals/72211.html.

Acknowledgments: This research leveraged data gained from a long-term ecosystem health research program led by the Grand Portage Band of Lake Superior Chippewa (GPBLSC) and the University of Minnesota. The GPBLSC is a federally recognized Indian tribe in extreme northeastern Minnesota and proudly exercises its rights to food sovereignty through subsistence hunting and fishing. Moose and deer are primary subsistence food used by the Anishinaabeg (people) of Grand Portage Band historically and presently and thus sets the context for this paper examining the impact of predators on disease transmission between the two cervid species. The GPBLSC is a sovereign indigenous nation that owns the data used in this manuscript. Those data are protected under the principles of data sovereignty [see T. Kukutai, J. Taylor, *Indigenous Data Sovereignty: Toward an Agenda* (ANU Press, 2016; https://library.oapen.org/handle/20.500.12657/31875)] and are shared under a data sharing and ownership agreement with the University of Minnesota for analysis and publication of

scientific products: see S. A. Moore, T. M. Wolf, D. A. Travis (2015). Data Sharing and Ownership Agreement for the Research Project "Building a One Health Research Collaboration between UMN and Grand Portage Indian Reservation" between the Grand Portage Band and the Regents of the University of Minnesota, on behalf of its College of Veterinary Medicine, Department of Veterinary Population Medicine. Retrieved from the University of Minnesota Digital Conservancy (https://hdl.handle.net/11299/213279). The Grand Portage Band has invested heavily in the acquisition of these important and sensitive data for the good of the Tribe. In maintaining ownership of these data, the Band ensures that any future western scientific products that emerge from these data integrate and reflect the cultural priorities of the Band. The Grand Portage Band is unwilling to make the data publicly available as they show where culturally important and subsistence species occur on the reservation. In recognizing the spirit of the intent for others to be able to access the data independently and replicate the results presented in this manuscript or leverage the data for new scientific discoveries, the Band offers that interested parties may request permission through DRUM repository (https://conservancy.umn.edu/drum) to use these data. Any entities that receive these data will be required to meet the terms of a data ownership and sharing agreement.

Funding: This study was supported by the Minnesota Environment and Natural Resources Trust Fund, as recommended by the Legislative-Citizen Commission on Minnesota Resources; the U.S. Fish and Wildlife Services Tribal Wildlife Grant Program; the U.S. Bureau of Indian Affairs; the U.S. EPA Great Lakes Restoration Initiative; the Minnesota Zoo Ulysses S. Seal Conservation Fund; the Indianapolis Zoo Conservation Grant; and the Van Sloun Foundation.

Author contributions: Conceptualization: L.G.R.O.-S., S.A.M., J.D.F., L.E.E., and T.M.W. Capture and data collection: S.A.M., E.J.I., Y.C.-I., and T.M.W. Data analyses: L.G.R.O.-S. and J.D.F. Writing—original draft: L.G.R.O.-S., W.J.S., and T.M.W. Writing—review and editing: L.G.R.O.-S., S.A.M., W.J.S., J.D.F., T.G., E.J.I., Y.C.-I., L.E.E., and T.M.W. **Competing interests:** The authors declare that they have no competing interests. **Data and materials availability:** All data needed to evaluate the conclusions in the paper are present in the paper and/or the Supplementary Materials. Data simulated from the original, methods and code are available in a persistent repository at the following URL (https://hdl.handle.net/11299/225296). See Acknowledgments section about details on data sharing regarding Indigenous Data Sovereignty.

Submitted 22 May 2021
Accepted 3 November 2021
Published 22 December 2021
10.1126/sciadv.abj5944